Operando Spatially and Time Resolved XAS Study on Zeolite Catalysts for Selective Catalytic Reduction of NO_x by NH_3

Dmitry E. Doronkin[†], Maria Casapu[†], Tobias Günter[†], Oliver Müller[‡], Ronald Frahm[‡], Jan-Dierk Grunwaldt[†]*

[†]Institute for Chemical Technology and Polymer Chemistry, KIT, Kaiserstr. 12, D-76131 Karlsruhe, Germany

[‡]University of Wuppertal, Gaußstr. 20. D-42097 Wuppertal, Germany

ABSTRACT. The structure of iron and copper sites during the selective catalytic reduction (SCR) of NO_x by NH_3 and related reactions (NH_3-adsorption/oxidation, NO-oxidation) has been elucidated by spatially- and time-resolved X-ray absorption spectroscopy (XAS) along the catalyst bed over Fe-containing BEA and ZSM-5 zeolites as well as Cu-SAPO-34 silicoalumophosphate. Strong gradients of the Fe and Cu oxidation state are present along the catalyst bed for the processes involving NH_3 and NO_x (SCR) and less pronounced for NH_3 oxidation, whereas the catalyst state in the NO_x containing feed resembles that of a catalyst exposed to air. The variation in the oxidation state is strongly correlated to the concentration of NH_3 and is more pronounced in the presence of NO_x. For temperatures higher than 250 °C the Fe and Cu sites in the beginning of the catalyst bed stay in partially reduced state, whereas they are more oxidized in the later zones where NH_3 and NO concentrations decrease. For temperatures lower than 250 °C the reverse effect is seen for Fe zeolites with the beginning of the catalyst bed more oxidized than the end which is tentatively attributed to strong NH_3 inhibition. The obtained data allows to conclude that both NH_3 and NO_x are involved in a reaction over the corresponding transition metal site and its reoxidation is a rate-limiting step of the NH_3-SCR.

KEYWORDS. Selective Catalytic Reduction, operando spectroscopy, X-ray absorption spectroscopy, spatially resolved, exhaust gas catalysis, zeolites

I. INTRODUCTION.

The removal of NO_x from the exhaust of diesel-powered vehicles can be achieved using ammonia in the so-called selective catalytic reduction (SCR) reaction. The main reaction ("Standard SCR") proceeds highly selective according to the equation (1) [1]:

$$4\ NO + O_2 + 4\ NH_3 \rightarrow 4\ N_2 + 6\ H_2O. \qquad (1)$$

As catalysts for mobile applications Fe- and Cu-containing zeolites and related materials are used [2]. They maintain high activity in a broad range of exhaust gas temperatures and are rather stable under hydrothermal conditions [3]. However, for further improvement mechanistic aspects of the SCR reaction and the structure of the active sites need to be uncovered, in particular in order to pave the way for kinetic modeling required for designing the aftertreatment system and for appropriate control algorithms.

Presently, the mechanism is still controversially discussed and several competing mechanisms of NO_x–SCR by ammonia over iron and copper sites have been proposed [4 - 6]. Many of these mechanisms claim the rate-determining step being oxidation of a reduced metal site by oxygen but in some schemes oxidation of NO to NO_2 is considered to be the rate-determining step [5]. Moreover, different sequences of steps leading to the reduction of metal site are proposed. Apostolescu et al. [4] suggest reduction of Fe^{3+} to Fe^{2+} to result from a dissociative adsorption of ammonia on that site. Metkar [5] and Ruggeri [6] propose the Fe^{3+} to Fe^{2+} reduction to originate from the oxidation of NO to the reactive intermediate HONO, whereas Metkar et al. [5] underline the necessity of the reaction between NH_3 and HONO on iron which leads to the freeing up of these sites and to the formation of Fe^{2+} with lower coordination numbers. In contrast, Ruggeri et al. [6] propose the spillover of HONO or its desorption as NO_2 as the process yielding Fe^{2+}. In the case of ammonia excess it can adsorb on both Fe^{3+} and Fe^{2+} blocking the subsequent NO adsorption,

Fe^{2+} reoxidation and, consequently, decreasing the overall SCR efficiency. This phenomenon is common for Fe-zeolites and is referred to as NH_3 inhibition [5 - 7].

The SCR catalysts have already been extensively investigated by a variety of in-situ techniques including X-ray absorption spectroscopy (XAS) [8 – 10]. A variation of Fe oxidation state was observed as a function of gas mixture and temperature for Fe-BEA catalysts [8 – 10]. Nevertheless, in all studies the structure was determined in a global manner, i.e. by monitoring the whole catalyst bed. The importance of spatially resolved studies has been outlined earlier for other reactions [11, 12], in particular, the catalytic partial oxidation of methane [13, 14]. A change of a catalyst red-ox state in a certain region of the catalyst bed due to the occurrence of the catalytic process in this region has been evidenced also for oxidation of CO [15]. The spatially-resolved UV-Vis study proved its applicability during a study of deactivation of Cr/Al_2O_3 catalyst for the dehydrogenation of propane [16]. Gradients in the surface concentrations of surface and bulk NO_x species were found and described for a NO_x storage-reduction (NSR) catalyst using Raman and diffuse-reflectance Fourier-transformed IR (DRIFT) spectroscopy [17]. In a few other cases a possible effect has been speculated on due to temperature and reactant concentration gradients [8, 18]. In fact, strong concentration gradients in the gas phase composition have recently been found by probing the gas phase in a channel of a honeycomb SCR catalyst [19]. Hence, the structural characteristics and dynamics obtained so far by in situ XAS for the Fe and Cu sites correspond either to an average of working and not working regions [8, 9] or only describe one part of the catalyst bed [8, 18, 20].

In this paper we report for the first time an *operando* spatially- and time-resolved X-ray absorption spectroscopy study of several NO_x SCR zeolite and zeotype catalysts including one commercial zeolite to describe a representative series of materials applied in the automotive

diesel exhaust aftertreatment. The main goal of the study is to further understand the mechanism of the SCR process by revealing and describing structural variations in the catalyst along the reactor bed while the gas composition changed due to the SCR reactions (NO_x and NH_3 reacted towards N_2 and H_2O). Complementary XAS spectra were also recorded during NH_3 and NO oxidation which accompany the SCR or are believed to be a part of this process [21].

II. EXPERIMENTAL SECTION

Sample preparation and characterization. 0.5%Fe-BEA and 2%Fe-BEA were obtained by incipient wetness impregnation of H-BEA zeolite (Si/Al ratio = 12.5, Clariant) with appropriate amount of $Fe(NO_3)_3 \cdot 9H_2O$ (VWR). After impregnation the catalysts were dried overnight at 80 °C and calcined for 4 h at 550 °C in static air. 0.84%Fe-BEA catalyst (0.84 wt.% Fe, 1.76 wt.% Al, Clariant) was used as received. Based on the UV-Vis spectra, EXAFS and catalytic data, the 0.5%Fe-BEA has mainly isolated monomeric Fe species and the 2%Fe-BEA – both isolated monomeric Fe species and inactive Fe_xO_y oligomers [8].

The 1.33%Fe-ZSM-5 catalyst was synthesized by liquid ion-exchange of NH_4-ZSM-5 zeolite (Si/Al ratio = 11, Clariant) with $FeCl_2$ (tetrahydrate, Sigma-Aldrich) as described in ref. [22]. For that purpose 5 g of zeolite was stirred in 500 ml of 0.05M solution of $FeCl_2$ under nitrogen flow for 24h. After that the solid was filtered, dried for 2 h at 120 °C and calcined for 5 h at 550 °C in static air.

Cu-SAPO-34 (3.48 wt.% Cu) was obtained using liquid ion-exchange of hydrothermally synthesized SAPO-34 [3]. First, 29.5 g aluminium isopropoxide (Sigma-Aldrich) was mixed with 48 g of deionized water and stirred for 1 h. At the same time 16.1 g H_3PO_4 (85 wt.% aq. solution, VWR), 60.7 g TEAOH (35 wt.% aq. solution, Alfa Aesar) and 4.5 g Ludox (Aldrich) were

mixed and stirred for 30 min. In the next step two solutions were mixed together and HCl (VWR) was added dropwise to adjust pH to 7. The slurry was then transferred to 200 ml Teflon-lined autoclave and heated statically for 24 h at 190 °C in an oven. After this the solid was recovered by decantation, washed with 800 ml deionized water, dried at 80 °C overnight and calcined for 8 h at 550 °C in static air. The SAPO-34 structure was confirmed using XRD.

As-prepared H-SAPO-34 was first exchanged to NH_4^+ form. For this purpose 6 g of the silicoalumophosphate was immersed and stirred in 500 ml of 0.5M solution of NH_4NO_3 (Merck) for 1 h at 80 °C and afterwards filtered and washed with deionized water. The procedure was repeated 3 times. Cu^{2+} was introduced by ion exchange of NH_4-SAPO-34 with 0.05 M $Cu(CH_3COO)_2$ (Merck, stirring for 24 h at 20 °C, 5 g solid per 500 ml solution). The obtained solid was filtered, dried overnight at 20 °C and calcined at 550 °C for 2 h.

The metal content in all ion-exchanged catalysts was determined using atomic absorption spectroscopy (AAS). For the measurements 30 mg of a sample was melted with 180 mg of $Li_2B_4O_7$ in Pt crucible at 1000 °C for 30-45 min, then cooled down, dissolved in 20 ml 2.5% citric acid at 80 °C and diluted by 100 ml deionized water.

Catalysis (laboratory setup). The catalytic data were obtained using laboratory setup with a fixed-bed plug-flow quartz tube reactor (8 mm i.d.) in the steady-state mode. The temperature was controlled using an Eurotherm 2416 controller with a K-type thermocouple. The catalyst temperature was measured by a second thermocouple touching the quartz wool plug next to the catalyst. Gases were dosed by individual mass flow controllers via heated lines to get a mixture of 0-1000 ppm NO, 0-1000 ppm NH_3, 10% O_2, 5% H_2O, and He balance. Water vapor was

obtained by feeding a required amount of H_2 (diluted with He) together with O_2 through an oxidation catalyst. Reaction products were analyzed by an MKS MultiGas 2030 FTIR analyzer.

The catalyst samples (49 mg for Cu-SAPO-34 and 80 mg for Fe-zeolites, sieve fraction 200-300 μm) were diluted by 800 mg quartz pearls to get 1 cm bed length and GHSV was 130 000 h^{-1} for Fe-zeolites and 330 000 h^{-1} for Cu-SAPO-34. The NO_x conversion during SCR was calculated using concentrations of NO and NO_2 (the amount of N_2O was normally negligible and max. 2% of total inlet NO_x for 0.84%Fe-BEA at 330 °C) and coincided well with NH_3 conversion below 400 °C.

XAS study. Next, *operando* XAS measurements were conducted on these samples at selected positions of the catalyst bed in transmission mode at the SuperXAS beamline of the SLS (Swiss Light Source) using a fast oscillating Si (111) channel cut crystal allowing to record fast data by the QEXAFS mode [23 - 25]. The catalyst (sieve fraction 100-200 μm) was placed in a 1 – 1.5 mm quartz capillary (20 μm walls) which served as a plug-flow reactor [26] heated by a hot gas blower (FMB Oxford). The catalyst response was followed between 185 – 550 °C in a gas stream of 25-40 ml/min (giving GHSVs similar to the laboratory reactor) containing 0 – 1000 ppm NO, 0 – 1200 ppm NH_3, 10% O_2, ~1.5% H_2O in He. The gases were mixed by individual mass flow controllers and water was fed via a saturator. The outlet gas composition was analyzed by online QMS (Hiden Analytical) and FTIR (MKS 2030) analyzers. The gas flow going to the FTIR analyzer was additionally diluted by 250 ml/min N_2. The FTIR data was used to determine NO_x and NH_3 conversions. The temperature of the catalyst bed was verified via an additional experiment with a K-type thermocouple set in place of a catalyst. For time and spatially resolved measurements the catalyst bed (ca. 10 mm length) was divided into 5 zones (spaced evenly from

inlet to outlet, referred to as positions 1 to 5) and XAS spectra were collected at all positions with an X-ray beam of about 200 μm x 200 μm.

Linear combination analysis (LCA) of the XANES data was performed using ATHENA program from the IFFEFIT package [27]. The reference spectra for fitting Fe oxidation state were obtained earlier during H_2-TPR of a Fe-ZSM-5 zeolite [28]. For fitting Cu oxidation state the spectrum of Cu^+ was chosen out of the series of Cu-SAPO-34 spectra recorded during H_2-TPR experiment (flow of 5% H_2 in He, ramp 3 °C/min) as the one having the highest intensity of the feature at 8982.5 eV. The reference XANES-TPR experiments were performed at ANKA synchrotron radiation source (XAS beamline) with the same setup as used for the *operando* measurements of SCR.

Fitting of the EXAFS data was done using ARTEMIS software (IFFEFIT) [27]. After Fourier transformation of the k^3-weighted EXAFS function between 2.5 and 7 $Å^{-1}$, data fitting was performed in R-space between 1 and 2 Å (corresponding to Fe–O or Fe–N shells). As a model compound, hematite was chosen and fitted with two Fe–O shells [29]. From this fit, $S^2_0 = 0.48$ was obtained and used for fitting the catalyst materials. In all fits ΔE_0 was kept the same for all scattering paths as well as the Debye–Waller factor for Fe–O backscattering.

III. RESULTS AND DISCUSSION

Catalytic activity. Fig. 1 shows the performance of the tested catalysts as measured in the laboratory plug-flow reactor. The obtained data qualitatively correspond to the conversion curves known for Fe (see for example ref. [8]) and Cu (see for example ref. [3]) zeolites and correlates with the data measured at the beamline during operando XAS studies (Fig. 2). The difference observed in the region of high conversions is due to the slip of the reagents in the laboratory test

bench (due to the catalyst dilution) which caused maximum NO_x conversion to be 85-90% instead of 98-100% observed in the literature [3, 8] and at the beamline.

Notably, 0.5%Fe-BEA and 2%Fe-BEA prepared by impregnation showed similar activity in all tests, which, together with the UV-Vis data (not shown here) and the previous results [8], indicates a high fraction of the SCR-inactive spectator Fe species in the 2%Fe-BEA.

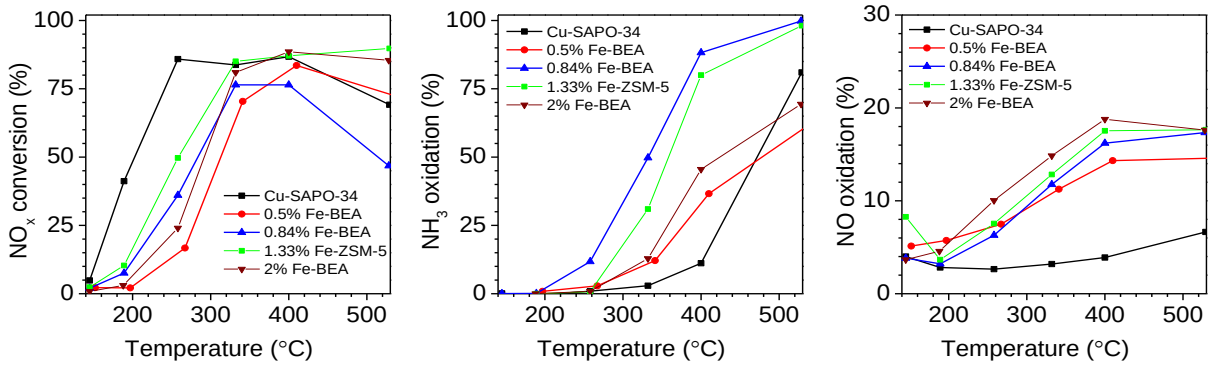

Figure 1. NO_x conversion obtained during SCR (left), NH_3 and NO oxidation correspondently (middle and right respectively) using the laboratory setup. Conditions: 1000 (0) ppm NO, 1000 (0) ppm NH_3, 5%O_2, 10% H_2O, He balance; GHSV = 130 000 h^{-1} (Fe-zeolites) and 330 000 h^{-1} (Cu-SAPO-34).

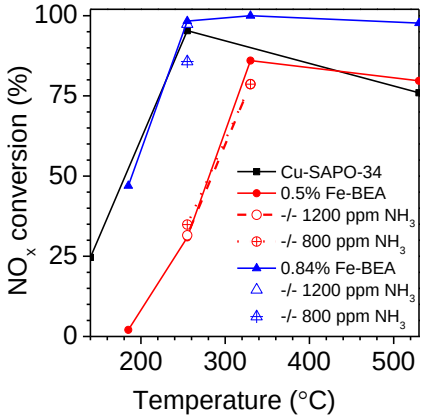

Figure 2. NO_x conversion obtained during SCR using the capillary microreactor at the synchrotron. Conditions: 1000 ppm NO, 1000 (1200, 800) ppm NH_3, 10%O_2, 1.5% H_2O, He balance; GHSV = 140 000 h^{-1} (Fe-zeolites) and 360 000 h^{-1} (Cu-SAPO-34).

Spatially-resolved XAS at Fe-K edge at high temperatures (T>250 ºC). During heating the catalysts under He or synthetic air dehydration of all Fe catalysts with the shift of the absorption edge towards lower energies was observed. This indicates a slight reduction and a change in coordination geometry which is in line with results reported earlier [8]. This effect was noticed independently of the probed reactor zone.

The introduction of the SCR gas feed caused a gradient of Fe oxidation state along the catalyst bed. Fig. 3a shows the XANES spectra recorded at different positions of the catalyst bed during SCR at 330°C over 0.5%Fe-BEA catalyst using 800 (top) and 1200 (bottom) ppm NH_3 together with 1000 ppm NO. With only moderate overall NH_3 inhibition effect even at NH_3/NO = 1.2, the NO_x conversion was 80 ± 3% for all used concentrations of NH_3. This almost equal NO conversion rate implies similar catalytic activity for different NH_3 concentrations in the gas phase, which is in line with previous kinetic studies on Fe-zeolites [30, 31]. A clear shift of the X-ray absorption edge towards lower energies is observed at the beginning of the catalyst bed relative to the end of the bed, which demonstrates the need to probe in a spatially-resolved manner. The pre-edge feature of the XANES spectra also changed with the centroid position shifting towards higher energies at the end of the catalyst bed which is also an indication of the reduction of Fe sites at the beginning of the catalyst bed and oxidation at the end [32]. The average oxidation state of the Fe sites at the probed position (Fig. 4) was evaluated by linear combination analysis using the reference spectra obtained during TPR of a Fe-ZSM-5 catalyst [28]. The results

indicate a clear impact of NH_3 concentration on the overall oxidation state which is, however, stronger at the inlet of the catalyst bed. These variations do not correlate only with the catalytic activity [17] but can be furthermore related to the local concentration of NH_3.

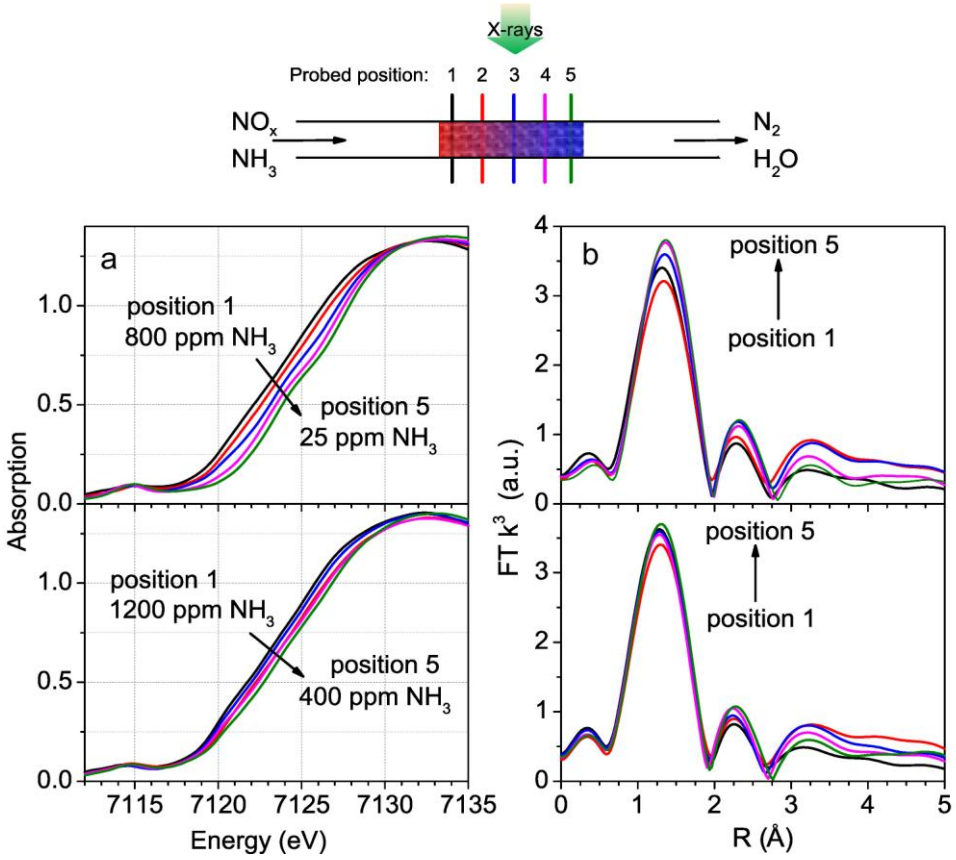

Figure 3. Comparison of (a) XANES and (b) Fourier transformed EXAFS data at Fe K-edge (k^3-weighed, k-range of 2–7 $Å^{-1}$, no phase-shift correction) at 800 ppm NH_3 (top Figures) and 1200 ppm NH_3 (bottom Figure) in the feed during SCR at 330 °C over the 0.5%Fe-BEA catalyst at five different points of the quartz microreactor (from the beginning to the end of the catalyst bed as indicated in the schematic Figure). Conditions: 1000 ppm NO, 800 (top) or 1200 (bottom) ppm NH_3, 10%O_2, ~1.5% H_2O, He balance; GHSV = 130 000 h^{-1}.

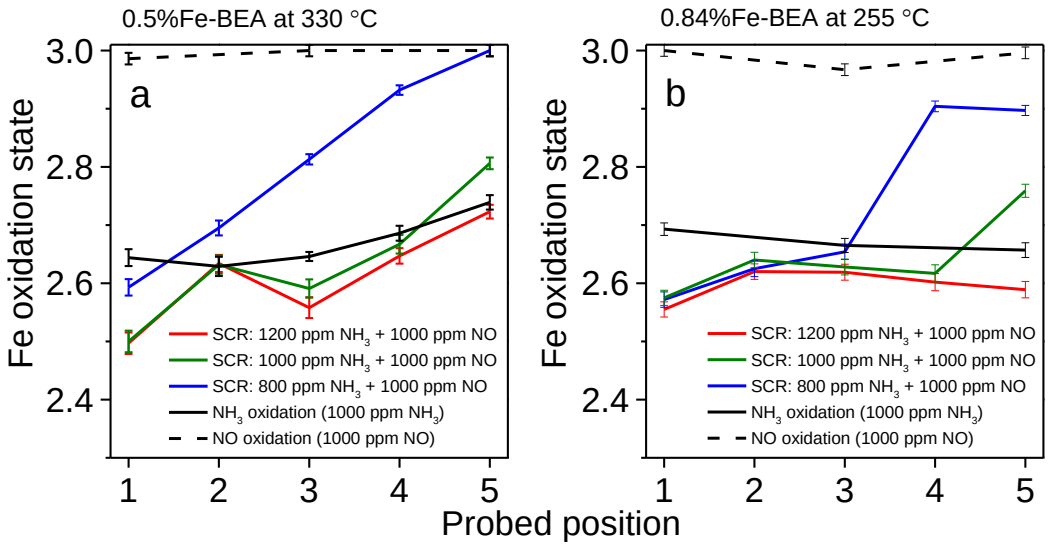

Figure 4. Average oxidation state of Fe sites in the 0.5%Fe-BEA and 0.84%Fe-BEA estimated from linear combination at the different positions in the catalyst bed during SCR, NH_3 and NO oxidation at 330 and 255 °C correspondently.

The same spatially-resolved study performed for the NH_3 oxidation reaction at 330 °C resulted in a similar gradient of the oxidation state (Fig. 5 shows the recorded XANES spectra and Fig. 4a – the Fe oxidation state). However, the standard SCR gas mixture (NH_3/NO=1) leads at 255 °C to slightly more reduced Fe sites for half of the catalyst bed as compared to the NH_3 oxidation conditions (shown clearer on the example of 0.84%Fe-BEA, Fig. 5b). In this region for the NH_3 excess gas mixture (NH_3/NO=1.2) after a pronounced drop at position 1 of the catalyst bed the oxidation state is slightly increasing and afterwards slowly decreases. At higher temperatures, the zone with more reduced Fe sites is shrinking towards the beginning of the catalyst bed due to an increased reaction rate. The same decrease of the more reduced catalyst zone was observed also for lower NH_3 concentrations and the opposite effect at NH_3/NO = 1.2. In contrast to the SCR and NH_3 oxidation processes, an average oxidation state of +3 ± 0.05 and no pronounced

gradient along the reactor was found during NO oxidation (Figs. 4a and 5) or the catalyst under air. However, one should also consider the lower reaction rates of the NH_3 and NO oxidation as compared to the SCR reaction at the studied temperatures.

Such pronounced gradients of the Fe-oxidation state during SCR were not only determined for 0.5%Fe-BEA (530, 330, 255 °C) and for 0.84%Fe-BEA (530, 330, 255 °C) but also for 1.33%Fe-ZSM-5 (probed for 530 and 330 °C). A less noticeable gradient of the same type was also observed for 2%Fe-BEA at 255 °C but no Fe reduction was found at higher temperatures. This is most probably related to the fact that the 2%Fe-BEA catalyst has a significant amount of Fe_xO_y spectator species [8] which do not change their structure during NH_3 adsorption at studied temperatures but contribute to the averaged oxidation state.

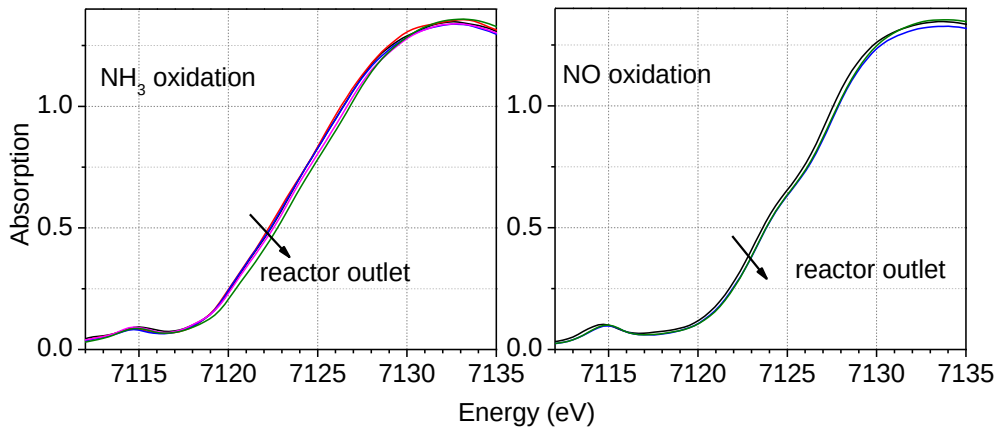

Figure 5. XANES spectra at Fe K-edge of the 0.5%Fe-BEA catalyst during NH_3 oxidation (left) and NO oxidation (right) at 330 °C. The spectra are measured at the different positions of the quartz microreactor (NH_3 oxidation: 5 points, NO oxidation: 3 points from inlet to outlet in the direction of an arrow). Conditions: 0 ppm NO, 1000 ppm NH_3, (right) or 1000 ppm NO, 0 ppm NH_3, (left), 10%O_2, ~1.5% H_2O, He balance; GHSV = 130 000 h^{-1}.

The Fourier transformed EXAFS spectra of the studied zeolites (Fig. 3b) show backscattering between 1 and 2 Å due to light elements (O or N) in the first coordination shell [33]. The small contributions appearing at about 2.5 Å may result from backscattering on Si or Al atoms from the zeolite framework or (less probable) from the second Fe atom [8, 33, 34]. In agreement with the white line evolution in the XANES region, changes were also observed in the EXAFS region of the spectra during SCR. In the catalyst zone with more oxidized iron due to a lower NH_3 concentration the Fe sites demonstrated a higher amplitude of the first coordination shell at about 1.4 Å (uncorrected for phase shift) which indeed correlates with a higher number of O neighbors. This effect is shown in Fig. 3b for 0.5%Fe-BEA under SCR with 800 and 1200 ppm NH_3 at 330 °C and the results of the EXAFS fitting (fit with two Fe-O shells, based on the Fe_2O_3 model [8]) are given in Fig. 6. Due to the low data quality to fit 4 parameters (bond distances and coordination numbers for two Fe-O shells) the results are reported with high error bars (0.3–0.8 in the case of coordination numbers) and should be taken with care and, thus, rather as trends. Together with a slight increase in the coordination number towards the end of the catalyst bed (more oxidized Fe) smaller bond distances were observed for both fitted Fe-O shells which is in line with an increased charge of a central Fe atom. The same overall trend was also clearly determined for 1.33%Fe-ZSM-5 and 0.84%Fe-BEA.

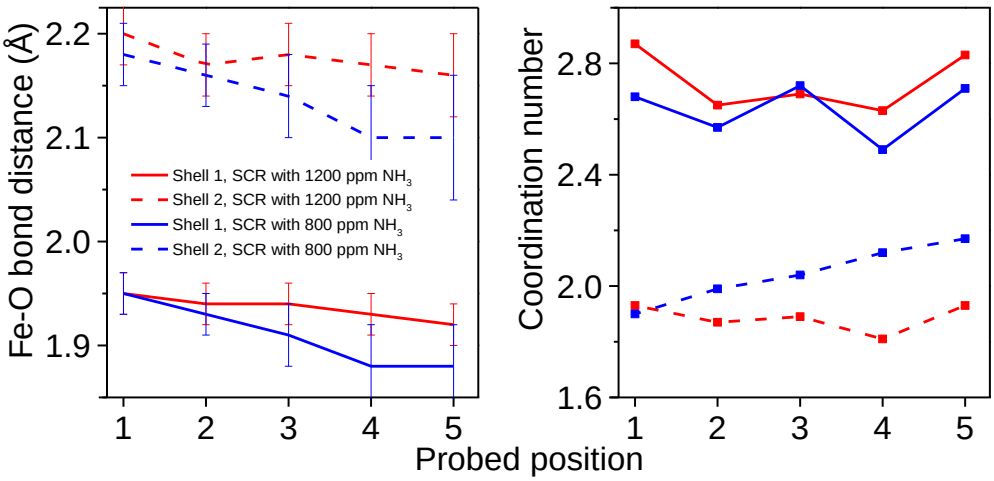

Figure 6. Fe-O bond distances and coordination numbers (error ±0.3–0.8) resulting from fitting of the EXAFS spectra of 0.5%Fe-BEA measured under SCR conditions with 800 and 1200 ppm NH_3 at 330 °C.

Thus, the observed shift of the absorption edge towards lower energies (Fig. 3a) with the corresponding variations in the coordination sphere can be attributed to the partial reduction of Fe sites in the probed zone by reaction between adsorbed NH_3- [4] and NO_x- derived species [5, 6]. Furthermore, the change of the oxidation state along the catalyst bed uncovered the so far suggested chemistry of the "Standard" and partially "Fast–SCR" reactions over Fe-zeolite catalysts. Although not prominently determined for the applied testing conditions in the overall catalyst performance (Fig. 2), still a noticeable NH_3 inhibition effect was observed along the catalyst bed at all studied temperatures. Especially localized at the inlet of the catalyst bed this phenomenon could be explained either by NH_3 adsorption and blocking of Fe^{3+} sites [6] and / or NH_3 adsorption and stabilization of Fe^{2+} sites which were initially formed in the SCR process or by the formation of ammonia-nitrate/nitrite ad-species stable in the presence of high NH_3 concentration (position 1, Fig. 3a). This fits well with the overlapping of the Fe oxidation state

points at 800, 1000 and 1200 ppm NH_3 dosage for the 0.84%Fe-BEA at 255°C and of the 1000 and 1200 ppm points at 330°C for the 0.84%Fe-BEA (lower NH_3 inhibition). Further downstream in the catalyst bed the NO and possibly the NO_2 present in the gas stream (due to NO oxidation in the pipe) react following the "Standard" or the "Fast–SCR" mechanisms.

For an excess of NO and without NH_3 inhibition the catalyst gets oxidized simultaneously with NH_3 consumption (Fig. 4a, 800 ppm NH_3 curve). For higher NH_3 concentration after a small increase of the oxidation state at position 2 of the catalyst bed the oxidation state is decreasing again. The increase of the Fe^{3+} concentration could be explained by NH_3 depletion at the catalyst surface and thus freeing/oxidation of the Fe^{2+} sites due to the "Fast-SCR" reaction. The occurrence of the "Fast-SCR" prior to the "Standard" SCR reaction was previously demonstrated by FTIR monitoring the NO/NO_2 concentrations along a Fe-Beta zeolite monolith during SCR [19]. Due to the excess of NH_3 (decreasing towards the outlet on behalf of the parallel NH_3 oxidation reaction) but probably also as a result of reaction between NO and NH_3 at the Fe centers or oxidation of NO to reactive HONO followed by its desorption as NO_2 [6] or N_2 [5] after reaction with NH_3, Fe^{2+} is progressively formed and stabilized in the standard SCR – NH_3 oxidation zone of the catalyst bed (Fig. 4b positions 3 and 4 for 1000 ppm NH_3 dosage). The length of this region directly depends on NH_3 concentration and reaction temperature, the catalyst being oxidized as soon as ammonia is consumed.

Spatially-resolved XAS at Fe-K edge at low temperatures (T<250 ºC). While the data measured at high temperatures showed partial reduction of Fe sites in the beginning of the catalyst bed, the spatially-resolved data measured at 185 ºC shows an opposite trend and the average iron oxidation state is higher (Fig. 7). In this case, the beginning of the catalyst bed is

more oxidized than the end of the bed in spite of the highest concentration of NH_3 as reductant in the beginning of a catalyst bed. This was observed for 0.84%Fe-BEA (Fig. 7), 2%Fe-BEA, and 1.33%Fe-ZSM-5. However, note that at this temperature even in the absence of oxygen the reduction of the Fe sites by NH_3 is limited [8]. Furthermore, the oxidation of NH_3 and the conversion of NO are rather small. Nevertheless, the first one or two positions of the catalyst bed with Fe-zeolites measured during SCR or NH_3 oxidation (Fig. 4) seem to correspond to NH_3 coordinated to the Fe^{3+} sites which hinders the access of NO for the first case (NH_3 inhibition) [35]. The rest of the catalyst bed is used for the SCR process with the most active zone of the catalyst bed shifted towards the end as demonstrated with our spatially-resolved data. Thus, analogous to the high temperature results, the oxidation state of Fe decreases simultaneously with the increase of NO conversion, subsequently to the NO adsorption at the Fe sites as the NH_3 concentration is decreasing (e.g. Fig. 4b positions 3 – 5 of the catalyst bed).

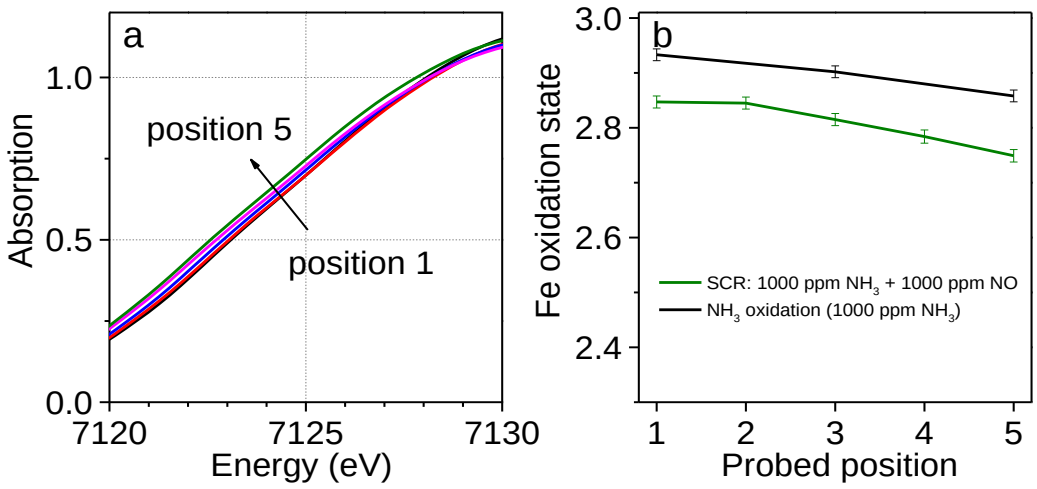

Figure 7. (a) XANES spectra and (b) estimated average oxidation state of Fe sites measured on the 0.84%Fe-BEA at the different positions in the reactor during SCR at 185 °C; in (b) additionally measured during NH_3 oxidation.

Spatially-resolved XAS at Cu-K edge. As the spatially resolved detection of the structure and oxidation state turned out to be very important for the Fe-based zeolites, we also studied Cu-SAPO-34 as an example of Cu-based SCR catalysts. Also in this case we selected a catalyst with high amount of monomeric isolated species and a high performance in SCR. Once again, the XAS measurements at different positions of the catalyst bed during SCR and NH_3 oxidation at 255 °C (95% NO_x conversion) resulted in different intensity of the Cu K-edge features around 8986 eV and especially at about 8982.5 eV in the XANES region (Fig. 8a). The feature at 8982.5 eV appears due to the 1s→4p transition in Cu^+-species [36]. Besides, a weak pre-edge associated with dipole-forbidden quadrupole-allowed 1s→3d transitions can be distinguished around 8977.5 eV which indicates the presence of Cu^{2+} sites [37, 38]. The increased intensity at 8982.5 eV at the beginning of the catalyst bed corresponds to a higher fraction of reduced Cu sites. For the determination of the average Cu oxidation state in the Cu-SAPO-34 during SCR a linear combination analysis was performed in the 8970 – 9045 eV range. In this case spectra of Cu-SAPO-34 measured during temperature-programmed reduction by H_2 were taken as Cu^{2+} and Cu^+ references in the same way as in ref. [37]. The results shown in Fig. 8a evidence an overall partial reduction of the catalyst which is in line with the data obtained during the SCR of NO over Cu-SSZ-13 [20]. However, only in the present case the oxidation state was measured in a spatially resolved manner which indicates a stronger reduction of Cu at the beginning of the catalyst bed. Consistent with the data obtained for Fe-zeolites, the FT EXAFS spectra of the Cu-SAPO-34 (Fig. 8b) demonstrate also a slightly lower coordination number due to light elements (O or N) in the first coordination shell [33] of Cu sites in the front zone of the catalyst bed. However, in this case the profile of the oxidation state gradient reflects more that of 0.5%Fe-

BEA zeolite tested at 300°C under insufficient NH_3 dosage conditions (800 ppm) with a smooth increase of the oxidation state simultaneously with the NO conversion advance. This is in line with the higher basic character of the Cu sites and thus less NH_3 adsorption (no inhibition). Furthermore, the activity of the Cu-SAPO-34 being less sensitive to the NO/NO_2 ratio [39], the small NO_2 amount which could be formed in the dosage pipes had no significant impact on the overall conversion and consequently on the oxidation state.

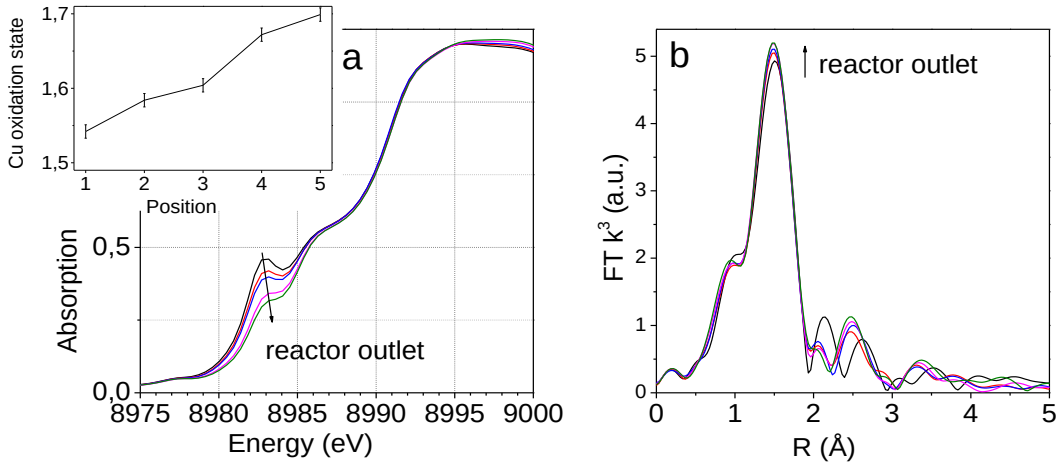

Figure 8. (a) XANES and (b) Fourier transformed EXAFS spectra recorded at Cu K-edge (k^3-weighed, k-range of 3–11 $Å^{-1}$, no phase-shift correction) from the Cu-SAPO-34 catalyst during SCR at 255 °C at the different points of the capillary (5 points, from the beginning to the end of the catalyst bed in the direction of the arrow). Inset shows average Cu oxidation state estimated from LCA-analysis depending on the probed part of the reactor. Conditions: 1000 ppm NO, 1000 ppm NH_3, 10%O_2, ~1.5% H_2O, He balance; GHSV = 360 000 h^{-1}.

Nevertheless, the gradient of Cu oxidation state can also be correlated with the local concentration of NH_3 and the presence of NO_x along the catalyst bed. Similar to 0.5%Fe-BEA,

0.84%Fe-BEA and 1.33%Fe-ZSM-5 samples, the increase of the average oxidation state derived from XANES is also present during NH_3 oxidation and does not appear during NO oxidation (Fig. 9). Under NH_3 and O_2 the characteristic spectral feature of Cu^+ is much weaker, which could be also due to the lower NH_3 oxidation activity at this temperature. This indicates that analogous to the Fe-exchanged zeolites the SCR process occurs probably via a copper complex which involves the adsorption of both NH_3 and NO on one or two sites (as e.g. NH_3 – Cu^+ – NO^+) or that the reaction of adsorbed NH_3 with surface nitrites and nitrates leads to an overall more pronounced reduction. Consistent with the data obtained for Fe-zeolites, in this case the Fourier transformed (FT) EXAFS spectra (Fig. 8b) demonstrated a slightly lower coordination number at Cu sites in the catalyst bed inlet zone. Further studies are currently pursued in our laboratory to directly probe the nature of the ligands around iron and copper.

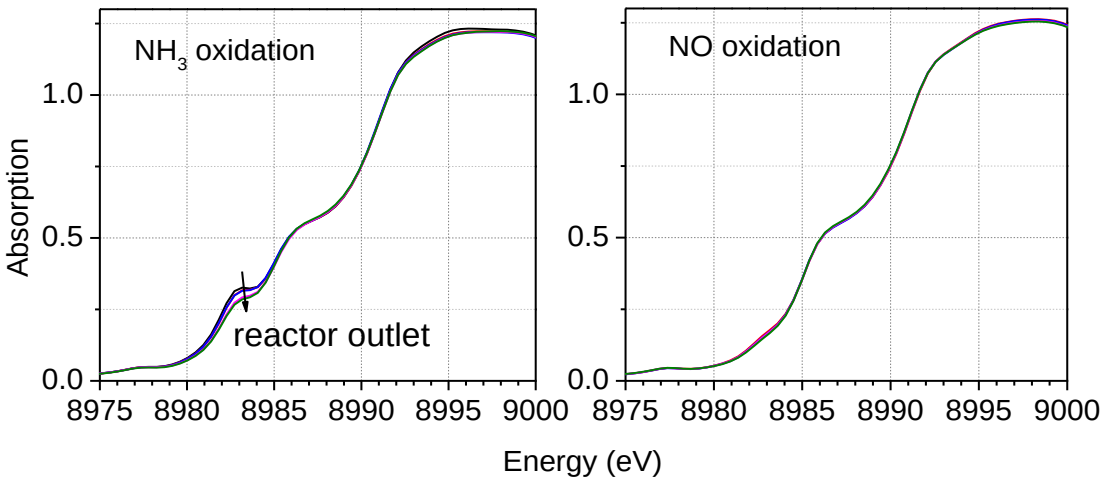

Figure 9. XANES spectra at Cu K-edge of the Cu-SAPO-34 catalyst during NH_3 oxidation (left) and NO oxidation (right) at 255 °C. The spectra are measured at the different points of the microreactor (5 points, from inlet to outlet in the direction of arrow). Conditions: 1000 ppm NO, 800 (top) or 1200 (bottom) ppm NH_3, 10%O_2, ~1.5% H_2O, He balance; GHSV = 360 000 h^{-1}.

Time- and spatially-resolved XAS during transient supply of NH_3.

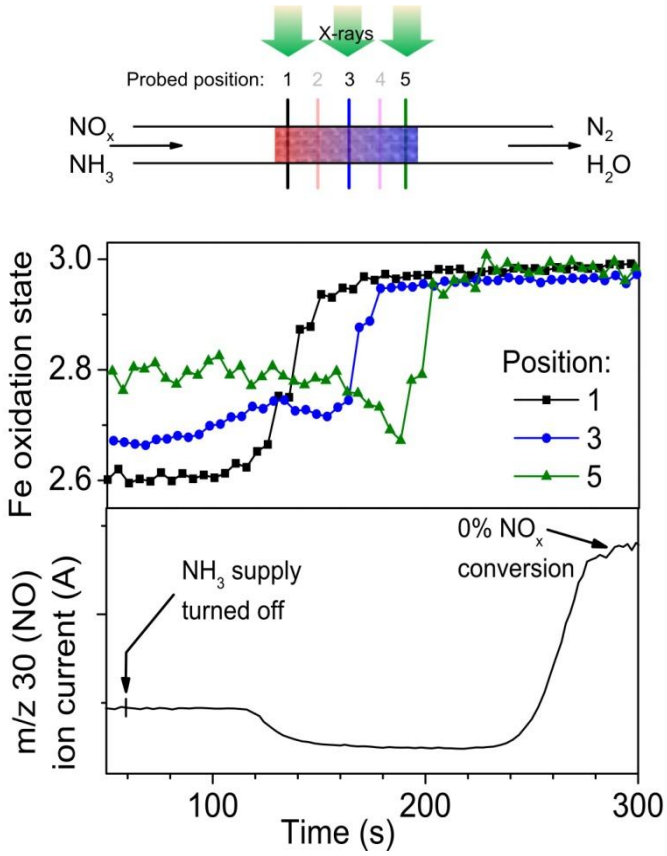

Figure 10. Evolution of average Fe oxidation state in the 0.84%Fe-BEA catalyst at the beginning, middle and end of the catalyst bed during removal of NH_3 from the SCR feed at 330 °C. Conditions: 1000 ppm NO, 1000 ppm / 0 ppm NH_3, 10% O_2, ~1.5% H_2O, He balance; GHSV = 130 000 h^{-1}. Three transients were recorded with different points probed by the X-ray beam and then synchronized using MS and FTIR data.

Another important aspect of the SCR process is the transient supply of reagents, which is widely used for the determination of the reaction mechanism [5, 6] and also to substantially increase

NO_x conversion over Fe-zeolites [35]. In this respect, additional time-resolved studies under transient NH_3 supply were performed on Fe and Cu samples. The evolution of Fe oxidation state in different parts of the microreactor during removal of ammonia from the SCR feed at 255 °C on 0.84%Fe-BEA catalyst is presented in Fig. 10. With NH_3 in the feed the usual gradient of the Fe oxidation state along the catalyst bed has been observed with more reduced iron species towards the beginning and more oxidized sites towards the end. After turning off the ammonia supply (60 s and some induction period due to the "dead volume" of the setup) the expected increase in the NO_x conversion was observed [1, 5, 6, 35] (Fig. 10, bottom) accompanied by the oxidation of the Fe sites at the inlet of the catalyst bed. Along with the oxidation of the Fe sites at the inlet of the catalyst bed a mild reduction occurs for the Fe sites located at the middle of the catalyst bed later also followed by oxidation. The intermediate reduction is even more visible at the end of the catalyst bed. This demonstrates the storage of ammonia at the Brønsted sites of the zeolite and moreover indicates a spillover of the stored NH_3 to iron sites with further reaction there. This occurs particularly if sufficient amount of NO becomes available at the probed part of the catalyst bed (NO is not consumed in an upward region of the catalyst bed) and at the same time there is no excess of NH_3 to inhibit SCR. Consequently, the generation of the Fe^{2+} sites due to the SCR is accelerated at these catalyst bed positions. After depletion of the stored ammonia along the catalyst bed all zones become fully oxidized (Fe^{3+}) and NO_x removal fully stops with approx. 20% NO being converted to NO_2.

Discussion. Spatially and time-resolved XAS investigations of different metal-exchanged zeolites catalyzing NO_x removal uncovered a pronounced variation of the oxidation state (the formation of Fe^{2+} and Cu^{+}) and coordination number at the Fe or Cu metal sites in the catalyst

bed during NH_3 oxidation and SCR. A strong dependency of the oxidation state gradients on temperature and NH_3 supply was demonstrated. These effects have been neglected in most of the previous studies by IR, UV-Vis, XAS and EPR although the presence of concentration gradients is known and have been recently measured by Spaci-MS and Spaci-FTIR [18]. Furthermore, the reduction of Fe^{3+} to Fe^{2+} during NO oxidation or due to the SCR and the inhibition effect of NH_3 during the standard and fast SCR reactions over Fe-zeolite SCR catalysts has been intensively discussed by several research groups [5, 6, 39].

Based on the results reported here, the associated catalytic data and previously published studies we can interpret the oxidation state gradients observed during NH_3 oxidation, the SCR process but not during the NO oxidation reaction as follows. The variation of the oxidation state along the catalyst bed seems to be a result of several processes including NH_3 adsorption and inhibition, NH_3 oxidation and NO_x reduction by NH_3 at the Fe sites. The same behavior was uncovered for Cu-SAPO-34 except the NH_3 inhibition effect. Under NO and O_2 the iron and copper sites are maintained in an oxidized state which could be due to the lower reaction rate of this process but also to the fast reoxidation in the absence of NH_3.

Below 250°C the blockage of the Fe^{3+} by adsorbed ammonia leads to the limited SCR activity of such catalysts as compared to the Cu-SAPO-34 or in general to the Cu-exchanged zeotype catalysts. This effect is very pronounced at the inlet of the catalyst bed. At higher temperatures (>250°C) which correspond to higher reaction rates an increase of the overall Fe^{2+} and Cu^{+} formation was evidenced, in the case of iron-zeolites the amount being strongly influenced by NH_3 concentration. Moreover, the degree of Fe and Cu reduction is higher under SCR conditions relative to NH_3 oxidation.

These results suggest the formation of Fe^{2+} and Cu^{+} as a consequence of the reaction between the adsorbed NH_x and NO_x on iron and copper sites as schematically shown in Scheme 1 and which fits well to the mechanism suggested by Metkar and co-authors [5]. This might further explain the decrease of the coordination number of Fe^{2+} sites (Figs. 3b and 6) as a consequence of the reaction of NH_3 and HONO at the iron site with associated electron transfer including desorption of nitrogen leaving lower coordinated Fe^{2+}. Whereas Metkar et al. [5] suggest oxidation of NO over metal sites to be the rate-determining step, Ruggeri et al. [6] name reoxidation of Fe^{2+} to Fe^{3+} the slow step. The latter hypothesis is in agreement with our data e.g. evidenced by the abundance of Fe^{2+} in the active zone (see also Scheme 1).The intermediate species proposed in the mechanism scheme as resulting from NO and ammonia adsorption/reaction as well as the process steps were deduces considering the applied reaction conditions (e.g. gas mixture, temperature), the catalytic performance and XAS results but also in the light of previous theoretical (see e.g. [40]) and experimental studies [4 – 6, 41, 42] on similar Fe- and Cu-based SCR catalysts. However, their formation and also the mechanism steps need to be further elucidated in future by complementary techniques (e.g. X-ray emission spectroscopy).

Scheme 1. Suggested scheme for SCR of NO_x by NH_3 over metal-zeolites (on the example of Fe) as deduced from the present operando XAS data (NH_3 adsorption and spillover on the zeolite are not shown). Only ligands relevant for SCR are shown as there are always additional H_2O and NH_3 ligands completing the Fe coordination sphere.

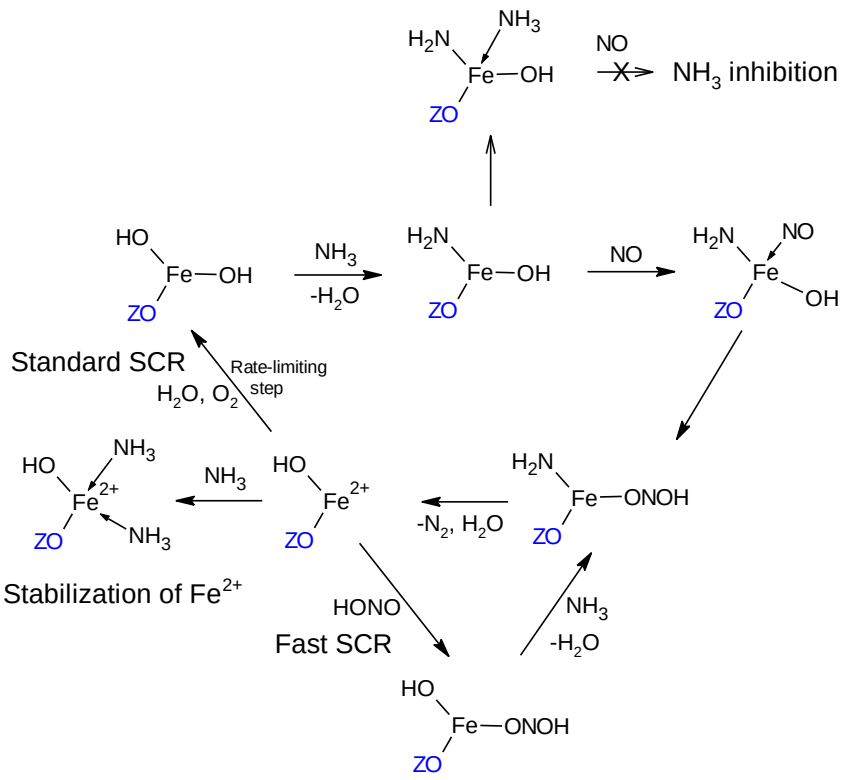

Furthermore, the suggested scheme describes the origin of the ammonia inhibition named by many authors [5, 6], i.e. the adsorption of NH_3 on Fe which does not leave any coordination site for the subsequent NO adsorption at low temperature (NH_3 blockage). Below 250°C, this phenomenon makes those sites inaccessible for further SCR reaction hindering the overall process before Fe reduction stage. In good agreement with the experimental results, this leads to a higher averaged Fe oxidation state in the NH_3-inhibited zone. Noteworthy, more oxidized inlet zone at low temperatures (Fig. 7) was not seen for Cu-SAPO-34 which corresponds well to the kinetic studies in literature which do not find an NH_3 inhibition effect for Cu zeolites [39].

The detrimental effects of higher NH_3 concentrations has also been identified at higher temperatures but in this case the adsorbed NH_3 stabilizes the Fe^{2+} sites at the beginning of the catalyst bed (blockage) and inhibits the reoxidation of Fe^{2+} to Fe^{3+} for the following catalyst

zones. Due to the higher reaction rate at these temperatures, this effect could not be observed in the overall catalyst performance.

Note that XAS uncovered only the formation and stabilization of Fe^{2+} and Cu^{+} sites and the stabilization of Fe^{3+} at low temperatures which are indicators of SCR and NH_3 inhibition, respectively. Other parts of the scheme still require further experimental proof. Besides, the existence of the depicted species may also depend on the actual conditions, e.g. NO may react from the adsorbed state at low temperature [43] and approach NH_x from the gas phase at high temperature [30], furthermore, the sequence of NH_3 and NO_x adsorption on Fe and Cu sites may change depending on the temperature and gas concentrations.

IV. CONCLUSIONS

The state and distribution of Fe^{2+} and Cu^{+} sites in a zeolite matrix were, to our knowledge for the first time, characterized along the catalyst bed with analysis of gaseous reaction products under real SCR catalyst testing conditions, i.e. plug-flow reactor, relevant GHSVs and the presence of water. Moreover, this was done in a spatially- and time-resolved way as it is normally done for gaseous products using Spaci-MS or Spaci-FTIR, which allows to treat active sites as ordinary reaction products and use them as additional input parameters during modeling.

We have shown that the results and consequently the interpretation of the *in-situ* and *operando* XAS measurements on metal-containing zeolites during SCR and NH_3 oxidation strongly depend on the part of the catalyst bed being probed. By combining spatially- and time-resolved XAS with an on-line gas analysis we were able to identify and describe catalyst zones with high SCR activity, NH_3-inhibited zones and zones without SCR (e.g. due to the consumption of reagents) depending on the reaction temperature, gas flow and composition. And though averaged changes

of the catalyst bed under changing conditions were previously described by XAS, the knowledge of the trends is not less important. As an example, we have described two trends influencing the oxidation state of Fe: (i) SCR during which Fe^{3+} is reduced to Fe^{2+} leading to more reduced catalyst bed zones (Fig. 4a) and (ii) NH_3 inhibition which hinders the SCR process by blocking Fe^{3+} and stabilizing the Fe^{2+} species between 250 – 350°C and by blocking the Fe^{3+} sites at lower temperatures. Such information cannot be derived by techniques that provide integral data on the whole catalyst bed.

The obtained results allowed us to propose several mechanistic conclusions and to draw a modified SCR mechanism. This information is of tremendous importance for designing future automotive catalysts and for microkinetic description and system modeling of the aftertreatment system, including appropriate control algorithms, and need to be elucidated by further complementary spatially resolved in-situ techniques.

AUTHOR INFORMATION

Corresponding Author

* Prof. Dr. Jan-Dierk Grunwaldt; Email: grunwaldt@kit.edu

Author Contributions

The manuscript was written through contributions of all authors. All authors have given approval to the final version of the manuscript.

Funding Sources

The Federal Ministry of Education and Research (BMBF) with project "In situ Nanoskop" (Project No. 05K10VK1) and project "ZeitKatMat" (05K13VK3) as well as the virtual Helmholtz-Institute VI-403.

Notes

The authors declare no competing financial interests.

ACKNOWLEDGMENT

This work was supported by the Federal Ministry of Education and Research (BMBF) project "In situ Nanoskop" (Project No. 05K10VK1), project "ZeitKatMat" (05K13VK3), and the virtual Helmholtz-Institute VI-403. We thank Paul Scherrer Institute (Villigen, Switzerland) for providing beamtime for this study at the SLS SuperXAS (X10DA) beamline. We gratefully acknowledge Dr. M. Nachtegaal for the assistance during the XAS measurements. We also thank Clariant for providing BEA and ZSM-5 parent zeolites, and 0.84%Fe-BEA catalyst used in this study. We are grateful to A. Beilmann for elemental analysis. The reference spectra for XANES analysis were measured at the ANKA synchrotron radiation source (KIT, Karlsruhe). The authors thank Dr. Stefan Mangold for the help during measurements.

REFERENCES

(1) Brandenberger, S.; Kröcher, O.; Tissler, A.; Althoff, R. The State of the Art in Selective Catalytic Reduction of NO_x by Ammonia Using Metal-Exchanged Zeolite Catalysts *Cat. Rev. - Sci. Eng.,* **2008**, *50*, 492-531.

(2) Johnson, T. Diesel Engine Emissions and Their Control. *Platinum Met. Rev.*, **2008**, *52*, 23-37.

(3) Fickel, D.W.; D'Addio, E.; Lauterbach, J.A.; Lobo R.F. The Ammonia Selective Catalytic Reduction Activity of Copper-Exchanged Small-Pore Zeolites. *Appl. Catal. B*, **2011**, *102*, 441-448.

(4) Apostolescu, N.; Geiger, B.; Hizbullah, K.; Jan, M.T.; Kureti, S.; Reichert, D.; Schott, F.; Weisweiler, W. Selective Catalytic Reduction of Nitrogen Oxides by Ammonia on Iron Oxide Catalysts. *Appl. Catal. B* **2006**, *62*, 104–114.

(5) Metkar, P.S.; Salazar, N.; Muncrief, R.; Balakotaiah, V.; Harold, M.P. Selective Catalytic Reduction of NO with NH_3 on Iron Zeolite Monolithic Catalysts: Steady-State and Transient Kinetics. *Appl. Catal. B* **2011**, *104*, 110–126.

(6) Ruggeri, M.P.; Grossale, A.; Nova, I.; Tronconi, E.; Jirglova, H.; Sobalik, Z. FTIR In Situ Mechanistic Study of the NH_3-NO/NO_2 "Fast SCR" Reaction over a Commercial Fe-ZSM-5 Catalyst. *Catal. Today* **2012**, *184*, 107–114.

(7) Kröcher, O.; Devadas, M.; Elsener, M.; Wokaun A.; Söger N.; Pfeifer M.; Demel Y.; Mussmann L. Investigation of the Selective Catalytic Reduction of NO by NH_3 on Fe-ZSM5 Monolith Catalysts. *Appl. Catal. B* **2006**, 66, 208-216.

(8) Høj, M.; Beier, M.J.; Grunwaldt, J.-D.; Dahl, S. The Role of Monomeric Iron during the Selective Catalytic Reduction of NO_x by NH_3 over Fe-BEA Zeolite Catalysts. *Appl. Catal. B* **2009**, 93, 166-176.

(9) Maier, S.M.; Jentys, A.; Janousch, M.; Bokhoven, J.A.; Lercher, J.A. Unique Dynamic Changes of Fe Cationic Species under NH_3-SCR Conditions. *J. Phys. Chem. C* **2012**, *116*, 5846-5856.

(10) Klukowski, D.; Balle, P.; Geiger, B.; Wagloehner, S.; Kureti, S.; Kimmerle, B.; Baiker, A.; Grunwaldt, J.-D. On the Mechanism of the SCR Reaction on Fe/HBEA Zeolite. *Appl. Catal. B* **2009**, *93*, 185–193.

(11) Weckhuysen, B.M. Chemical Imaging of Spatial Heterogeneities in Catalytic Solids at Different Length and Time Scales. *Angew. Chem. Int. Ed.* **2009,** *48*, 4910-4943.

(12) Grunwaldt, J.-D.; Wagner, J.B.; Dunin-Borkowski, R.E. Imaging Catalysts at Work: A Hierarchical Approach from the Macro- to the Meso- and Nano-scale. *ChemCatChem* **2013**, *5*, 62-80.

(13) Stötzel, J.; Frahm, R.; Kimmerle, B.; Nachtegaal, M.; Grunwaldt, J.-D. Oscillatory Behavior during the Catalytic Partial Oxidation of Methane: Following Dynamic Structural Changes of Palladium Using the QEXAFS Technique *J. Phys. Chem. C* **2012**, *116*, 599-609.

(14) Korup, O.; Goldsmith, C.F.; Weinberg, G.; Geske, M.; Kandemir, T.; Schlögl, R.; Horn, R. Catalytic Partial Oxidation of Methane on Platinum Investigated by Spatial Reactor Profiles, Spatially Resolved Spectroscopy, and Microkinetic Modeling. *J. Catal.* **2013,** *297*, 1-16.

(15) Singh, J.; Nachtegaal, M.; Alayon, E.M.C.; Stötzel, J.; van Bokhoven, J.A. Dynamic Structure Changes of a Heterogeneous Catalyst within a Reactor: Oscillations in CO Oxidation over a Supported Platinum Catalyst. *ChemCatChem* **2010**, *2*, 653–657.

(16) Nijhuis, T.A.; Tinnemans, S.J.; Visser, T.; Weckhuysen, B.M. Towards Real-Time Spectroscopic Process Control for the Dehydrogenation of Propane over Supported Chromium Oxide Catalysts. *Chem. Eng. Sci.* **2004**, *59*, 5487-5492.

(17) Urakawa, A.; Maeda, N.; Baiker, A. Space- and Time-Resolved Combined DRIFT and Raman Spectroscopy: Monitoring Dynamic Surface and Bulk Processes during NO_x Storage Reduction. *Angew. Chem. Int. Ed.* **2008**, *47*, 9256-9259.

(18) Deka, U.; Lezcano-Gonzalez, I.; Warrender, S.J.; Picone, A.L.; Wright, P.A.; Weckhuysen, B.M.; Beale, A.M. Changing Active Sites in Cu–CHA Catalysts: DeNOx Selectivity as a Function of the Preparation Method. *Micropor. Mesopor. Mater.* **2013**, *166*, 144-152.

(19) Luo, J.-Y.; Hou, X.; Wijayakoon, P.; Schmieg, S.J.; Li, W.; Epling, W.S. Spatially Resolving SCR Reactions over a Fe/zeolite Catalyst. *Appl. Catal. B* **2011**, *102*, 110–119.

(20) McEwen, J.-S.; Anggara, T.; Schneider, W.F.; Kispersky, V.F.; Miller, J.T.; Delgass, W.N.; Ribeiro, F.H. Integrated Operando X-ray Absorption and DFT Characterization of Cu–SSZ-13 Exchange Sites during the Selective Catalytic Reduction of NO_x with NH_3. *Catal. Today* **2012**, *184*, 129–144.

(21) Marban, G.; Fuertes, A.B. Kinetics of the Low-Temperature Selective Catalytic Reduction of NO with NH_3 over Activated Carbon Composite-Supported Iron Oxides. *Catal. Lett.* **2002**, *84*, 13-19.

(22) Long, R.Q.; Yang, R.T. Fe-ZSM-5 for Selective Catalytic Reduction of NO with NH_3: A Comparative Study of Different Preparation Techniques. *Catal. Lett.*, **2001**, *74*, 201–205.

(23) Frahm, R. New Method for Time Dependent X-ray Absorption Studies. *Rev. Sci. Instrum.* **1989**, *60*, 2515-2518.

(24) Singh, J.; Alayon, E.M.C.; Tromp, M.; Safonova, O.V.; Glatzel, P.; Nachtegaal, M.; Frahm, R.; van Bokhoven, J.A. Generating Highly Active Partially Oxidized Platinum during Oxidation of Carbon Monoxide over Pt/Al_2O_3: In Situ, Time-Resolved, and High-Energy-Resolution X-Ray Absorption Spectroscopy. *Angew. Chem. Int. Ed.* **2008**, *47*, 9260-9264.

(25) Grunwaldt, J.-D.; Beier, M.; Kimmerle, B.; Baiker, A.; Nachtegaal, M.; Griesebock, B.; Lutzenkirchen-Hecht, D.; Stotzeld, J.; Frahm, R. Structural Changes of Noble Metal

Catalysts during Ignition and Extinction of the Partial Oxidation of Methane Studied by Advanced QEXAFS Techniques *PCCP* **2009**, *11*, 8779-8789.

(26) Grunwaldt, J.-D.; Caravati, M.; Hannemann, S.; Baiker, A. X-ray Absorption Spectroscopy under Reaction Conditions: Suitability of Different Reaction Cells for Combined Catalyst Characterization and Time-Resolved Studies. *PCCP* **2004**, *6,* 3037-3047.

(27) Ravel, B.; Newville, M. ATHENA, ARTEMIS, HEPHAESTUS: Data Analysis for X-ray Absorption Spectroscopy Using IFEFFIT *J. Synchrotron Radiat.* **2005**, *12*, 537-541.

(28) Günter, T.; Casapu M.; Doronkin D.; Mangold S.; Trouillet V.; Augenstein T.; Grunwaldt, J.-D. Potential and Limitations of Natural Chabazite for Selective Catalytic Reduction of NO_x with NH_3. *Chem. Ing. Tech.* **2012**, *85*, 632-641.

(29) Manceau, A.; Combes, J.M. Structure of Mn and Fe Oxides and Oxyhydroxides: A Topological Approach by EXAFS. *Phys. Chem. Miner.* **1988**, *15*, 283–295.

(30) Amiridis, M.D.; Puglisi, F.; Dumesic, J.A.; Millman, W.S.; Topsøe, N.Y. Kinetic and Infrared Spectroscopic Studies of Fe-Y Zeolites for the Selective Catalytic Reduction of Nitric Oxide by Ammonia. *J. Catal.* **1993**, *142*, 572–584.

(31) Huang, H.; Long, R.Q.; Yang, R.T. Kinetics of Selective Catalytic Reduction of NO with NH_3 on Fe-ZSM-5 Catalyst. *Appl. Catal. A* **2002**, *235*, 241–251.

(32) Wilke, M.; Farges, F.; Petit, P.E.; Brown, G.E.; Martin, F. Oxidation State and Coordination of Fe in Minerals: An Fe *K*-XANES Spectroscopic Study. *Am. Mineral.* **2001**, *86*, 714-730.

(33) Zecchina A.; Rivallan, M.; Berlier G.; Lamberti, C.; Ricchiardi, G. Structure and Nuclearity of Active Sites in Fe-zeolites: Comparison with Iron Sites in Enzymes and Homogeneous Catalysts. *PCCP* **2007**, *9*, 3483-3499.

(34) Pirngruber, G.D.; Roy, P.K.; Prins, R. On Determining the Nuclearity of Iron Sites in Fe-ZSM-5 – a Critical Evaluation. *PCCP* **2006**, *8*, 3939–3950.

(35) Wallin, M.; Karlsson, C.J.; Skoglundh, M.; Palmqvist, A. Selective Catalytic Reduction of NO_x with NH_3 over Zeolite H-ZSM-5: Influence of Transient Ammonia Supply. *J. Catal.* **2003**, *218*, 354–364.

(36) Kau, L.-S.; Spira-Solomon, D.J.; Penner-Hahn, J.E.; Hodgson, K.O.; Solomon, E.I. X-ray Absorption Edge Determination of the Oxidation State and Coordination Number of Copper: Application to the Type 3 Site in Rhus Vernicifera Laccase and Its Reaction with Oxygen. *J. Am. Chem. Soc.* **1987**, *109*, 6433-6442.

(37) Alayon, E.M.C.; Nachtegaal, M.; Kleymenov, E.; van Bokhoven, J.A. Determination of the Electronic and Geometric Structure of Cu Sites during Methane Conversion over Cu-MOR with X-ray Absorption Spectroscopy, *Micropor. Mesopor. Mat.* **2013**, *166*, 131-136.

(38) Kappen, P.; Grunwaldt, J.-D.; Hammershøi, B.S.; Tröger, L.; Clausen, B.S. The State of Cu Promoter Atoms in High-Temperature Shift Catalysts — An in Situ Fluorescence XAFS Study. *J. Catal.* **2001**, *198*, 56–65.

(39) Colombo, M.; Nova, I.; Tronconi, E. A Comparative Study of the NH_3-SCR Reactions over a Cu-zeolite and a Fe-zeolite Catalyst. *Catal. Today* **2010**, *151*, 223–230.

(40) Brüggemann T.C.; Keil F.J. Theoretical Investigation of the Mechanism of the Selective Catalytic Reduction of Nitrogen Oxide with Ammonia on Fe-Form Zeolites. *J. Phys. Chem. C* **2011**, *115*, 23854–23870.

(41) Devadas, M.; Kröcher, O.; Elsener, M.; Wokaun, A.; Mitrikas, G.; Söger, N.; Pfeifer, M.; Demel, Y.; Mussmann, L. Characterization and Catalytic Investigation of Fe-ZSM5 for Urea-SCR. *Catal. Today* **2007**, *119,* 137-144.

(42) Wang, D.; Zhang, L.; Kamasamudram, K.; Epling W.S. In Situ-DRIFTS Study of Selective Catalytic Reduction of NO_x by NH_3 over Cu-Exchanged SAPO-34. *ACS Catalysis* **2013**, *3,* 871-881.

(43) Sun, Q.; Gao, Z.-X.; Chen, H.-Y.; Sachtler, W.M.H. Reduction of NO_x with Ammonia over Fe/MFI: Reaction Mechanism Based on Isotopic Labeling *J. Catal.* **2001**, *201*, 88–99.

TOC IMAGE

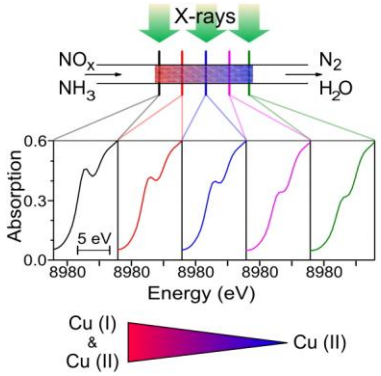
X-rays
NOx
NH3
N2
H2O
0.6
0.3
0.0
Absorption
5 eV
8980
8980
8980
8980
8980
Energy (eV)
Cu (I)
&
Cu (II)
Cu (II)